

3D Microstructural Finite Element Simulation of Martensitic Transformation of TRIP Steels

Abstract

In this paper the effects of deformation modes on martensitic transformation for TRIP steels which are composed of Ferrite, Bainite and Retained austenite are investigated in the view of the microstructural level. For this purpose the simulations are run for a synthetically generated microstructure which have 55% Ferrite, 35% Bainite and 10% Retained austenite. In the simulations tensile, biaxial and shear type deformation modes are considered. The results reveal that biaxially loaded microstructure has the maximum amounts of martensite phases at the end of the given deformation and the less martensite is occurred in the shear type loading condition.

Keywords

Martensitic transformation, TRIP, 3D microstructure generation, Finite element simulation

Serkan Toros^{a*}
Fahrettin Öztürk^b

^a Niğde Ömer Halisdemir University, Faculty of Engineering, Department of Mechanical Engineering, Niğde, Turkey. E-mail: serkantoros@ohu.edu.tr

^b Ankara Yıldırım Beyazıt University, Faculty of Engineering, Department of Mechanical Engineering, Ankara, Turkey. E-mail: fozturk@ybu.edu.tr

*Corresponding author

<http://dx.doi.org/10.1590/1679-78254533>

Received: September 22, 2017

In Revised Form: May 14, 2018

Accepted: May 28, 2018

Available Online: June 14, 2018

1. INTRODUCTION

Progression of the materials technology to meet the necessities and expectations of the automotive industry from the used materials in the structures increases expeditiously insomuch that specific materials are produced for the specific car components. One of the most commonly used material in the automotive structure is the Transformation-induced plasticity (TRIP) steel which is a kind of multiphase carbon steels. These steels exhibit the satisfactory combination of the strength and formability. The microstructure of TRIP steels consists of ferrite, bainite and untransformed retained austenite. According to the applied heat treatment process, a small amount of martensite can also be seen in the microstructure. The ductility and strength of the TRIP steels are provided by the transition of the unstable retained austenite to stable martensite phase with the plastic deformation that prevent the progression of the micro-cracks during the plastic deformation (Yu, Li et al. 2006). Besides that, since the volume of the martensite phase is higher than the retained austenite, additional hardening occurs in the surrounding phases (Jacques, Girault et al. 2001). This phenomenon leads to additional increase in the strength during the plastic deformation.

In literature, it is possible to find numerous experimental studies which are focused on the contribution of the transformation mechanisms of the retained austenite to mechanical properties like strength and ductility, and the process parameters that affect the quantity, morphology and stability of the austenite. Fu, Liu et al. (2013) investigated the effects of rolling and tension processes on the stability of the retained austenite during the plastic deformation. It is revealed that the martensitic transformation of the TRIP steels is affected from the applied deformation modes and the decaying rate of the austenite in the microstructure for the rolling operation is slower than the tension type deformation. He et al. (2012) studied the formability characteristic of the two different TRIP steels under dynamic and quasi-static strain rate levels. They showed that the elongation of the steels decreases with the increasing of the strain rate and this behavior is attributed to suppressing features of the strain rate on the martensitic transformation. Another parameter that affect the formability and strength level of the TRIP steels is the amounts of the retain austenite in the microstructure at the prior the forming operation. Generally, the higher retain austenite content in the microstructure means the higher formability during the stamping operations (Zrník, Stejskal et al. 2007a, Zrník, Stejskal et al. 2007b). Another parameter that affects the transformation of the retain

austenite is the size and shape of the austenite phases. Davut and Zaefferer (2012) demonstrated that larger austenite grains transform into martensite earlier than the smaller ones.

As can be understood from the experimental studies, the improvement in the mechanical properties of the materials are directly attributed to the microstructural evaluation with the performed manufacturing processes and their conditions. Recently, interactions between microstructure and mechanical properties can be comprehended by using the visualization techniques via optic microscope or SEM (scanning electron microscope) in two dimension (2D) and SEM-FIB (Focused ion beam) microscope for three dimension (3D). The obtained microstructure views are then analyzed in the view of the size, morphology and the quantity of the phases for the multiphase structures in order to determine the effects of these parameters. Optimization of the microstructures according to the required mechanical properties experimentally is very time consuming and costly. Therefore the researchers are focused on the numerical simulations of the material behaviors in the micro level due to the understanding of the effects of the aforementioned parameters that given above (Tjahjanto, Suiker et al. 2007, Sierra and Nemes 2008, Uthaisangskuk, Prah et al. 2009, Kubler, Berveiller et al. 2010, Kubler, Berveiller et al. 2011, Uthaisangskuk, Prah et al. 2011). Tjahjanto, Suiker et al. (2007) investigated the effects of microstructural parameters like initial volume fraction of the retained austenite, the elasto-plastic properties of the surrounding ferritic matrix, the crystallographic orientations of the ferritic and austenitic grains and finally the carbon concentration in the retained austenite on the overall mechanical response to applied deformation in a binary ferrite-austenite microstructural system. Although the generated system is able to mimic the transformation of the retained austenite partially, it is not sufficient to understand the interactions of the untransformed austenite with the other phase bainite.

Synthetically generated microstructures starts to become more convenient than the experimental works in view of the number of the parametric cases that affect the macroscopic response of the materials against the external factors (Alveen et al. 2013). These methods are generally used to link the microstructure with macroscopic behavior of the material. In literature there are several investigations about the modelling of the microstructures of the TRIP steels in 2D (Choi, Soulam et al. 2010) which are based on the monitoring of the microstructures via a suitable microscope and subsequently the meshing operation with an auxiliary software that is able to the segmentation of the phases or some other impurities. The generated and meshed microstructure images are then imported to proper finite element analysis software. Since the 2D microstructural modelling does not reflect the whole material's behavior, 3D modelling is essential. In the current study the martensitic transformation of TRIP800 advanced high strength steel is investigated via synthetically generated 3D microstructures. The main framework of the study includes the effects of different amounts of retained austenite on the transformation kinetics and macroscopic mechanical properties of the TRIP steel via the synthetically generated microstructures.

2. MICROSTRUCTURE GENERATION

Modelling of the synthetically generated microstructures by finite element software may provide us to comprehend the relation between microstructures and mechanical performance of the materials. In the study the effects of different amounts of the retained austenite in the structure is mainly investigated. The AFRL package DREAM.3D (Groeber, Ghosh et al. 2008a, Groeber, Ghosh et al. 2008b, Digital representation environment for analyzing microstructure in 3D, 2013. [http://dream3dbluequartznet.](http://dream3dbluequartznet)) is used to generate synthetic microstructures of TRIP steel from the statistics gathered in the characterization phase. The generated microstructures consists of the ferrite, bainite, retained austenite and martensite phases prior the finite element simulations. As a grain shape, the ellipsoid form is selected and their sizes are determined according to the optic microscope photo analyze results which is given in Figure 1. The grain sizes of the phases are varied from 1.8 to 3.7 μm for ferrite, 1.4 to 1.9 μm for bainite and 0.3 to 1.2 μm for retained austenite. Additionally, in case martensitic transformation is occurred with the heat treatment for the initial situation of microstructure, the grain size of the martensite phase is selected as varying between 0.36 and 0.42 μm .

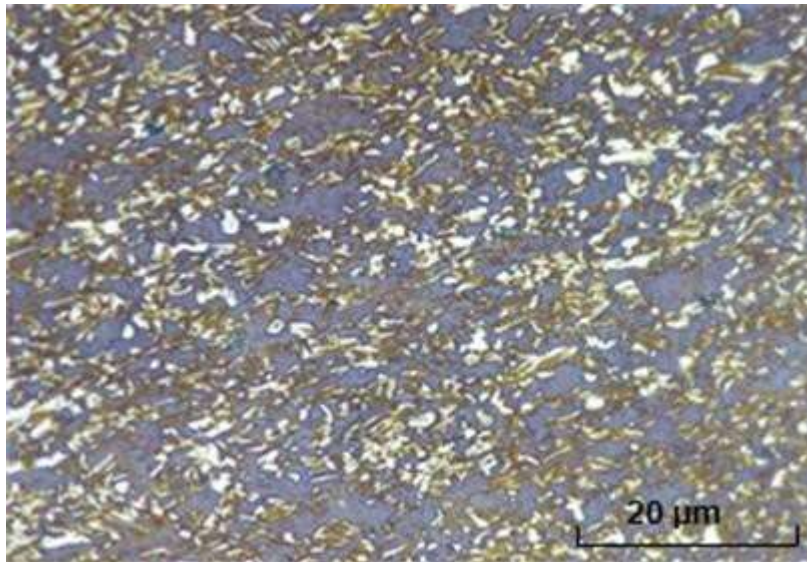


Fig. 1. The microstructural view of the TRIP 800 advanced high strength steels

In the software, it possible to create multiphase structures and the distribution and size of the grains are adjusted by the parameters μ and σ values which give the log-normal and the standard deviation of the grain size distribution. For the Ferrite phase μ and σ values are selected as 1 and 0.1, for bainite these values are 0.5 and 0.03, for the retained austenite -0.5 and 0.15 and finally for the martensite phase 0.95 and 0.02 respectively. The final microstructures are generated in the 25x25x25 voxel size and 6x6x6 μm.

The DREAM3D is able to generate the microstructures in the meshed shell format (.STL) which is need to be converted into the solid form. Therefore an auxiliary software needs to be used to generate the solid mesh which is more proper for the finite element simulation of the martensitic transformation. The conversion issue of the phases can be overcome via using the PPM which is a volumetric meshing routine developed by the Cornell Fracture Group. It is possible to create Abaqus ".inp" file of the generated microstructures in the ".stl" format. However it is more useful if the generated microstructures are converted to solid form phase by phase due to use the meshing algorithm of the each finite element software that is own. Therefore in the study FreeCAD software is used to convert the generated shell meshes in to the solid shape and exported as the ".step" format. Then the grouped phases are imported to COMSOL Multi-physics and analyses are evaluated.

In the study the effects of loading condition on martensitic transformation is investigated for a generated microstructure. A scenario about the distribution of the Ferrite, Bainite and Retained Austenite is selected as 55%, 35% and 10% respectively. The generated microstructure is given in Fig.2.

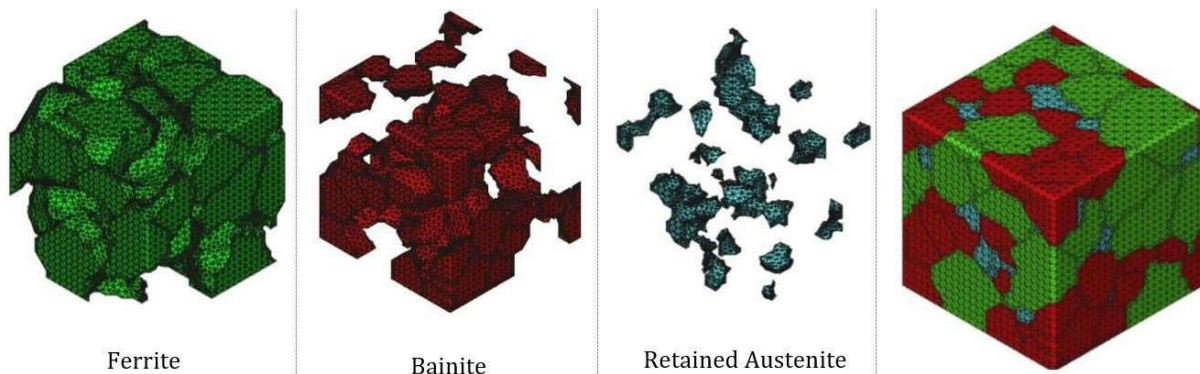


Figure 2. A generated microstructure according to the determined distribution by XRD

3. MODELING OF MARTENSITIC TRANSFORMATION

3.1. Dan's martensitic transformation model

The modelling of the martensitic transformation kinetics and implementation of the developed models into the proper finite element software is the key issue for the most researchers. One of the most commonly referred martensitic transformation model is the Olson and Cohen model (OC model) (Olson and Cohen 1975), in which the transformation can be represented with a three parameter model which gives the sigmoidal curve and the transformation is attributed to the onset of transformation to the intersection of the shear bands. The modelling works of the martensitic transformation kinetics can also be found in: (Stringfellow, Parks et al. 1992, Fischer, Oberaigner et al. 1998, Fischer, Reisner et al. 2000, Tomita and Iwamoto 2001).

The martensitic transformation with the given plastic deformation of the retained austenite can be given as follow;

$$f_m = 1 - \exp \left[-\beta \left(1 - \exp \left(-\alpha \bar{\varepsilon}_a^p \right) \right)^n \right] \quad (1)$$

where α is a temperature dependent parameter which is described as;

$$\alpha = -\alpha_1 T^2 - \alpha_2 T + \alpha_3 \quad (2)$$

T is the absolute temperature. The martensitic transformation rate from the retained austenite is decreased with the increasing temperature level. Therefore the parameter α is expected to decrease with the increasing of the temperature due to the increasing of the required mechanical driving force which is the level of the triggering of the martensitic transformation.

The parameter β is also stated in the Eq.1 in order to consider the effects of the shear bands which is the main responsible of the strain induced martensitic transformation during the plastic deformation of the retained austenite.

$$\beta = \beta_0 P = \frac{\bar{v}_m K}{(\bar{v}_{sb})^n} P \quad (3)$$

Stringfellow, Parks et al. (1992) than modified the OC model by contributing the effect of strain rate and the stress triaxiality on the martensitic transformation kinetics during the plastic deformation. In their study, the kinetics of the martensitic transformation explained by the occurring of the martensite embryos in the retained austenite. The existence rate of the martensite is attributed to rate of the shear bands. Additionally the shear band intersections which may act as the nucleation of the martensite is defined with a Gaussian cumulative probability distribution function P .

$$\frac{\dot{f}_m}{1-f_m} = \bar{v}_m \dot{N}_m = \bar{v}_m \left(P \dot{N}_{sb}^I + \dot{N}_{sb}^I \dot{P} H(\dot{P}) \right) \quad (4)$$

Due to the martensitic transformation is irreversible process, a Heaviside step function $H(P)$ is also used in Eq. 4. The Gaussian cumulative function can be described as below;

$$P(g) = \frac{1}{\sqrt{2\pi} S_g} \int_{-\infty}^g \exp \left[-\frac{1}{2} \left(\frac{\tilde{g} - \bar{g}}{S_g} \right)^2 \right] d\tilde{g} \quad (5)$$

\bar{g} and S_g are the mean and standard deviation of the normal distribution function respectively and temperature and stress triaxiality dependent g is the driving force which shows the required mechanic work for initiating the martensitic transformation in the microstructure.

$$g = g_0 - g_1 \Theta + g_2 \Sigma \quad (6)$$

where g_0 , g_1 , and g_2 are the constants and they reflect the magnitude of the temperature and triaxiality. Temperature has the negative effect on the martensitic transformation due to increase in the required mechanical

work which can be seen in Fig 3. The normalized temperature Θ that given in Eq.7 can be formulate with the upper martensitic transformation temperature level (M_d) and the lower temperature limit (M_s^σ) for the strain induced martensitic nucleation. Additionally in Eq. 6 the stress triaxiality (Σ) is also defined as the ratio of hydrostatic stress (mean stress) and Mises equivalent stress.

$$\Theta = \frac{T - M_s^\sigma}{M_d - M_s^\sigma} \quad (7)$$

In the calculation of the rate of martensitic embryo per unit volume of the retained austenite phases, the rate of the Gaussian probability function is necessary. Under isothermal conditions the rate of the probability function is given as follow.

$$\dot{P} = \frac{g_2}{\sqrt{2\pi}S_g} \exp\left[-\frac{1}{2}\left(\frac{\tilde{g} - \bar{g}}{S_g}\right)^2\right] \dot{\Sigma} \quad (8)$$

Finally the rate of the martensitic transformation is defined as follow with combination of the given equations;

$$\dot{f}_m = (1 - f_m)(A_f \dot{\bar{\epsilon}}^p + B_f \dot{\Sigma}) \quad (9)$$

where A_f is a parameter that describes the effects of the plastic deformation and B_f represents the probability of the martensite nucleation.

In this study, the martensitic transformation of the determined microstructures is modelled by the Dan et. al.'s model (Dan, Zhang et al. 2007) since it includes that the nucleation of the martensite phases in the microstructures is described through the contribution of the effects of the temperature increment with the given plastic deformation.

$$T = T_0 + \Delta T$$

$$\Delta T = \int_0^{\epsilon^p} \frac{\chi}{\rho C_p} \sigma(\epsilon^p) d\epsilon^p \quad (10)$$

$$\Delta \dot{T} = \frac{\chi}{\rho C_p} \sigma(\epsilon^p) \dot{\epsilon}^p$$

In the model, the probability rate of the martensitic nucleation is also comprise the effect of the temperature. Since the amounts of temperature can reach about 250 °C at high strain rates, it is essential to take into account the temperature rise in the modelling studies. The probability rate is given as;

$$\dot{P} = \frac{1}{\sqrt{2\pi}S_g} \exp\left[-\frac{1}{2}\left(\frac{\tilde{g} - \bar{g}}{S_g}\right)^2\right] (-g_1 \Delta \dot{T} + g_2 \dot{\Sigma}) \quad (11)$$

Similar to the Strinfellow's model the rate of the martensitic transformation is formulated as follow;

$$\dot{f}_m = (1 - f_m)(A \dot{\epsilon}^p + B \dot{\Sigma}) \quad (12)$$

where A and B parameters are represent the plastic strain contribution and martensite nucleation probability respectively.

$$A = r\alpha\beta P(1 - f_{sb})(f_{sb})^{r-1} - B_f \frac{g_1 \chi}{\rho C_p} \sigma(\bar{\epsilon}^p), \quad B = 2B_f \quad (13)$$

$$B_f = \beta(f_{sb})^r \frac{1}{\sqrt{2\pi}S_g} \exp\left[-\frac{1}{2}\left(\frac{\tilde{g}-\bar{g}}{S_g}\right)^2\right] H(\dot{P}), \quad \beta = \frac{C\bar{v}_m}{\bar{v}_l} \quad (14)$$

The given α parameter is described in terms of the material temperature, stress triaxiality and the strain rate effects which are the main dominant parameters on the martensitic transformation.

$$\alpha = \left(\alpha_0 + \alpha_1 T + \alpha_2 T^2 + \alpha_3 \Sigma\right) \left(\frac{\dot{\epsilon}^p}{\dot{\epsilon}_0^p}\right)^{\alpha_4} \quad (15)$$

Multiphase materials are generally modelled by the composite structure approaches. The value of the equivalent stress is determined according to the Miller and McDowell model which is developed for the two phase materials and adopted to triple phases.

The flow curves of the individual phases are represented with the following Swift equation in order to obtain stress strain data (Dan, Zhang et al. 2007). The model parameters are tabulated in Table 1 and model results are depicted in Fig 3.

$$\sigma = K(\epsilon_0 + \epsilon)^n \quad (16)$$

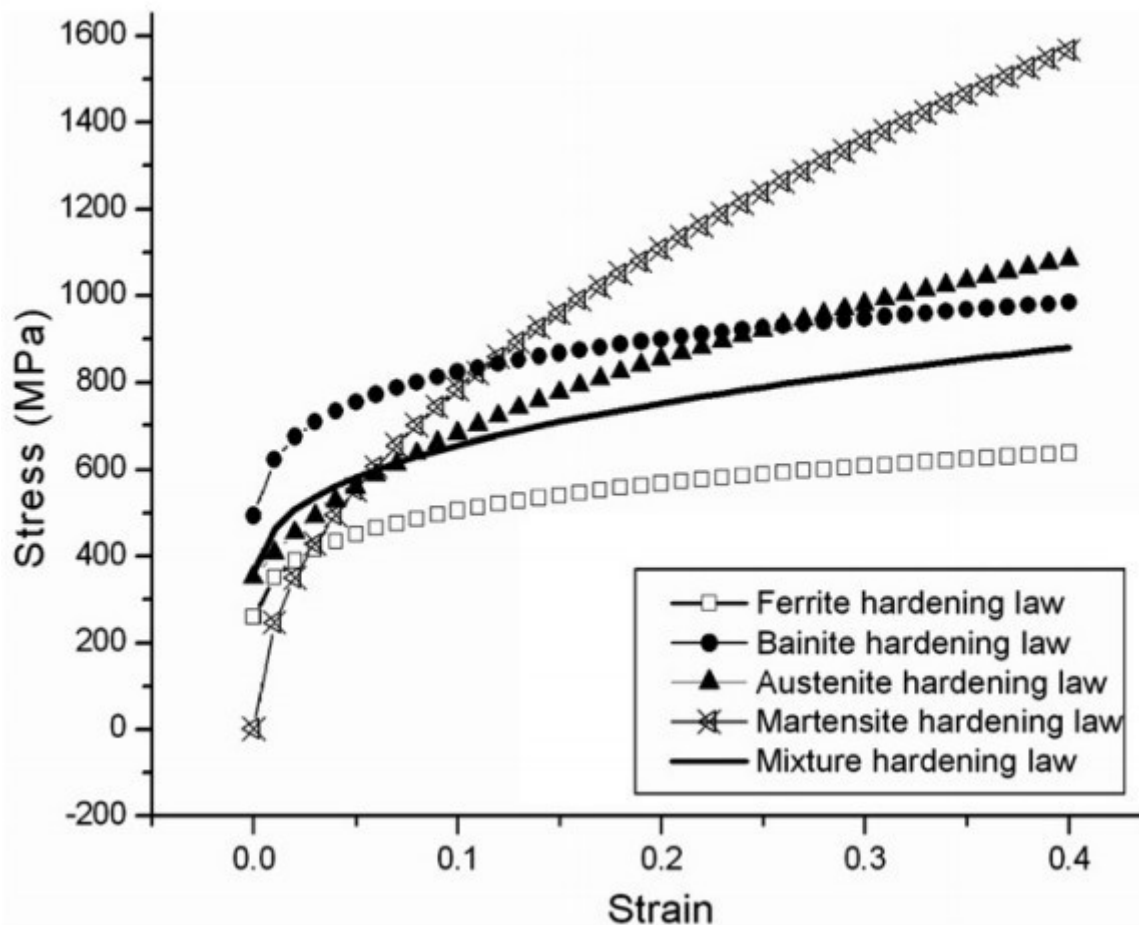


Fig. 3. Stress strain curves of the phases (Dan, Zhang et al. 2007)

Table 1. Flow curve model parameters for the phases

	K	n	ϵ_0
Ferrite	631	0.39	0.002
Bainite	1421	0.121	0.002
Retained Austenite	1490	0.44	0.02
Martensite	2498	0.29	1e-7

3.2. Boundary conditions

In the study, the created microstructure is depicted in Fig. 2 phase by phase. The selected boundary conditions are depicted in Fig. 4. As can be seen in the figures, three surfaces are selected as the symmetry boundary conditions and other surfaces are released. Additionally, a selected displacement is applied through the x direction on zx plane for tensile type deformation mode, z direction on zx plane for shear type deformation and finally z direction on xy plane and x direction on zx plane for biaxial deformation mode.

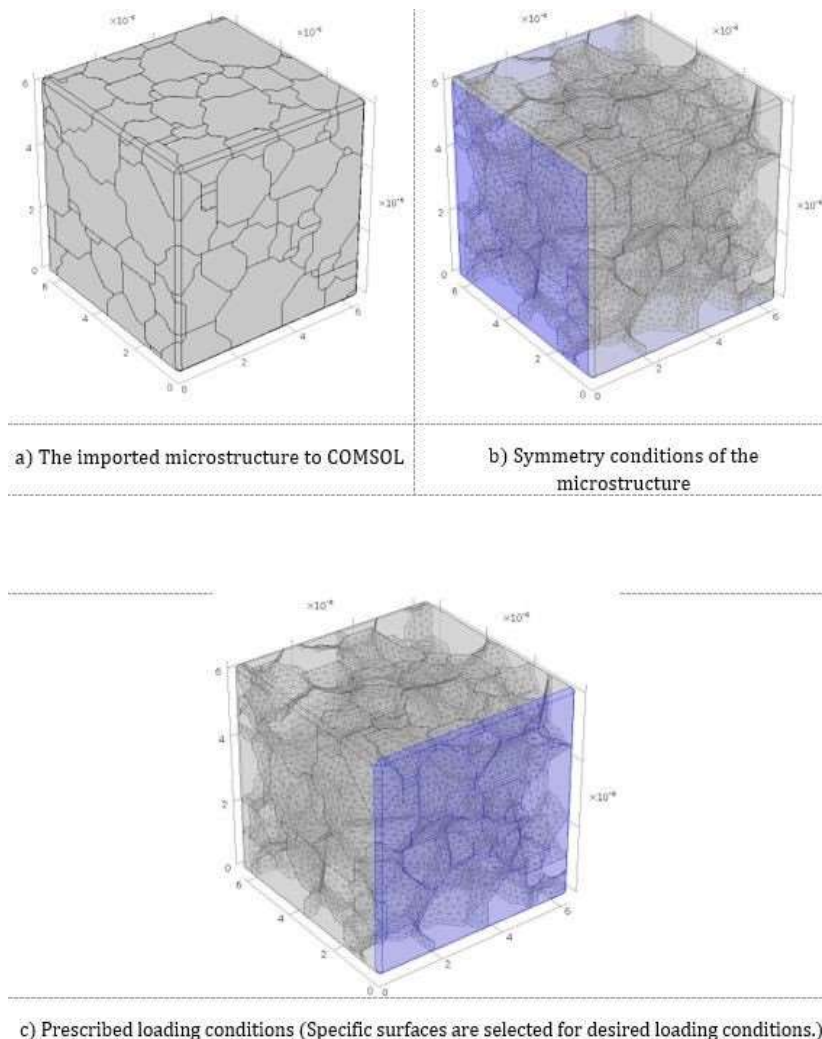


Fig 4. Boundary conditions and applied deformations through the selected surfaces.

4. RESULTS AND DISCUSSION

In Fig.5 the Dan transformation model is fitted to experimental martensitic transformation data belong to the tensile test and the model parameters are obtained. The experiments of martensitic transformation was carried out at room temperature and constant 0.0016 s^{-1} strain rate. As can be seen from the figure the model result is quite convenient with the experimental results. The model parameters are given Table 2.

Table 2. Dan martensitic transformation model parameters

α_0	α_1	α_2	α_3	α_4	
12.8023	0.0395	-0.0002	12.1105	0.7397	
g_0	g_0	g_0	β	σ_g	g
24.9153	-1.4352	152.8977	450.068	69.1625	-111.867

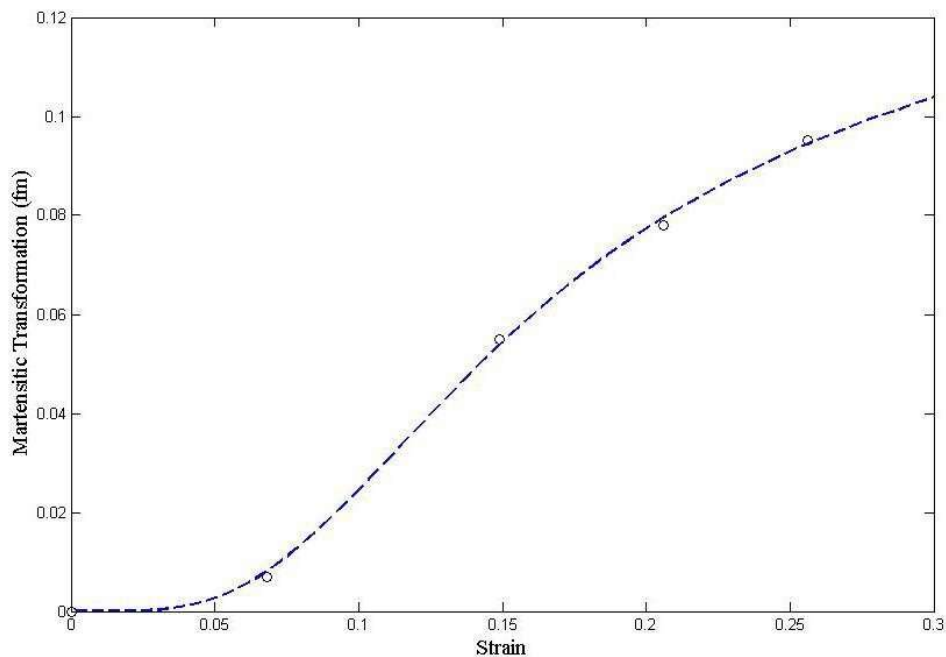


Fig. 5. Dan martensitic transformation model fitting to experimental data

Among the factors that affect the mechanical response of the TRIP steels, the amounts and shapes of the phases are the important issue for the selection of the right combination. Due to the experimental works which are very time consuming and non-economic, the synthetically generated microstructures help us to comprehend the material behavior for the selected cases. If any useful information can be obtain about the microstructures that need to be produced by this new approaches, it will find many application in the materials science.

In this study, the martensitic transformation mechanism under different loading conditions like tensile, biaxial and shear type deformation modes and its contribution to the mechanical response are modelled by using the synthetically generated representative volume elements (RVEs). Stress – strain relations for different deformation modes are given in Fig. 6. Firstly, the equivalent stress distributions on the retained austenite are depicted in Fig.7 for the selected loading conditions. The amounts of the prescribed strain value is selected as $0.3 \mu\text{m}/\mu\text{m}$ for all cases. As can be seen from the figure the maximum martensitic transformation on the created representative volume elements depicts some difference due to the contribution of the loading conditions. As reported before, the martensitic transformation depends on many conditions like the amounts of carbon concentration of the retained

austenite, loading modes, temperature, and strain rates. Since the modelling and simulation are very time consuming, in the study only the deformation modes' effects are investigated.

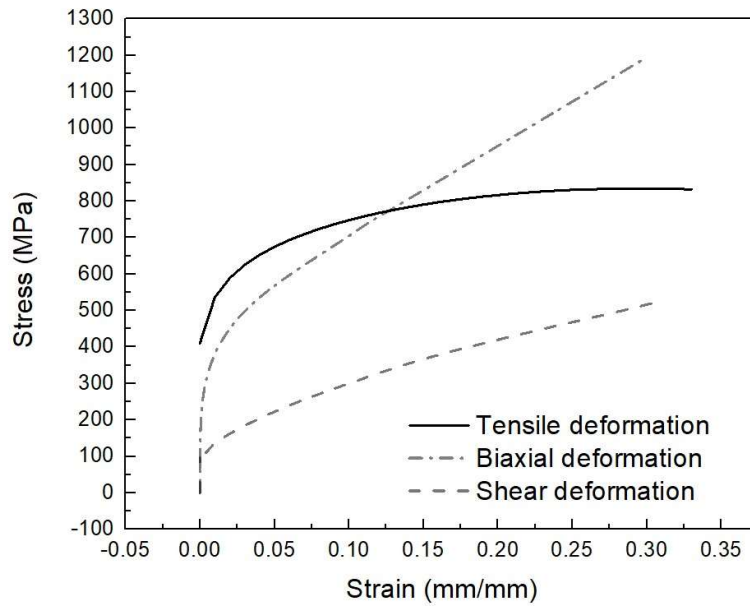


Fig. 6. Stress - strain relations for different deformation modes

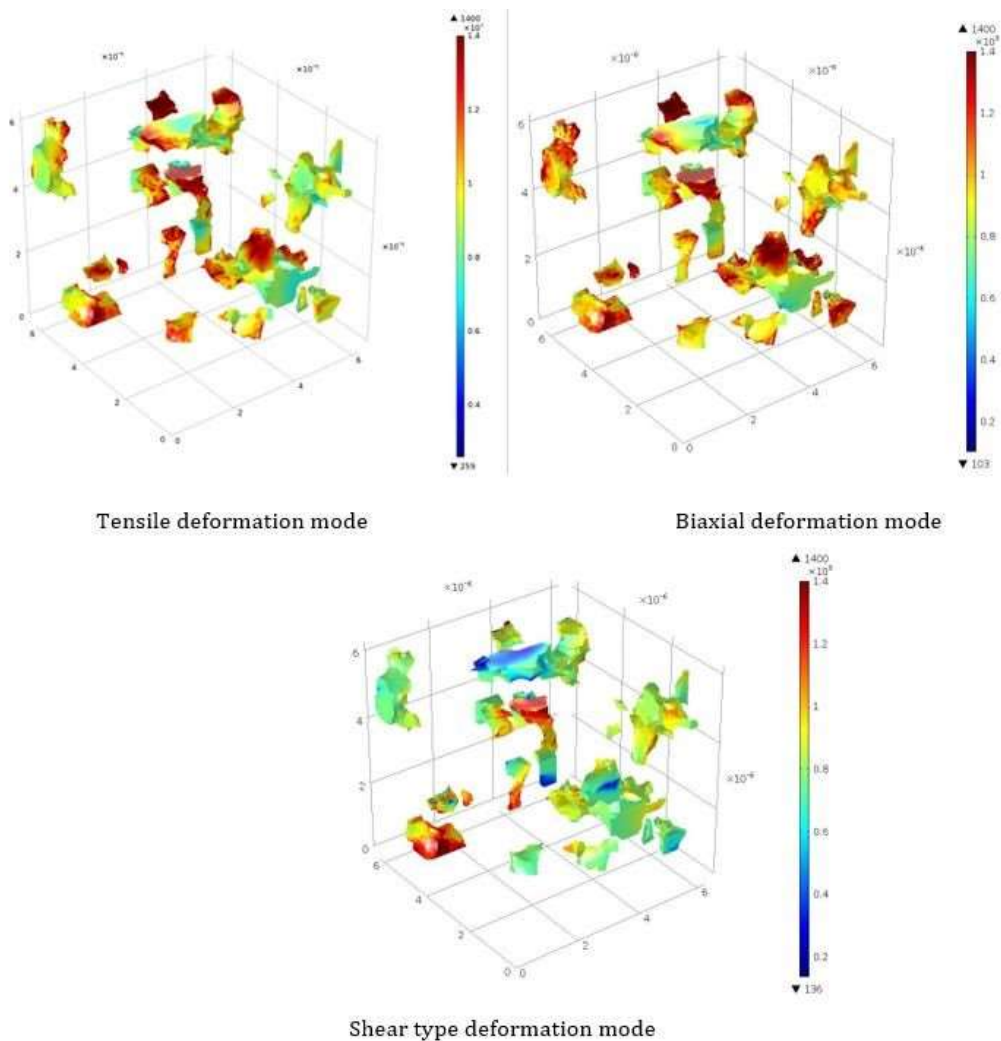


Fig. 7. The equivalent stress distribution

As can be understood from the stress distributions on the retained austenite depicted in Fig.7, the maximum stress distribution is more common for the biaxial loading conditions for the prescribed strain value. This is followed by the tensile loading and the shear type loading conditions. This situation can cause more martensitic transformation on the retained austenite. According to carried out experimental studies on the martensitic transformation for different loading conditions (Stringfellow, Parks et al. 1992), the obtained simulation results are very convenient with the experimental observations in the macro scale. Additionally the stresses in shear type loading conditions is less than the other two situation. When the model parameters that effect the martensitic transformation, are investigated, the drag force and the shear band creation are the important ones, which are directly related with the transformation kinetic of the retained austenite. The amounts of the martensitic transformation at the end of the given deformation for the prescribed conditions such as loading mode, temperature and strain rate, depends on these parameters. Among these conditions, the loading modes have the preferential effect for conventional stamping operations since they are carried out at room temperature frequently. The shear bands creations that triggered the martensitic nucleation in the microstructure can be obtained as continuously increased form through the given deformation. In addition, this increment is the highest when compared with the other loading conditions uniaxial and shear type deformations. Therefore, at the end of the prescribed deformation, the amount of the martensitic transformation reached to highest value.

The martensitic transformation for the selected cases are depicted in Fig. 8. The results are also convenient with the obtained stress distributions. As can be seen from the figure the maximum transformation is obtained from the biaxial loading conditions and 86% of the retained austenite is transformed into the martensite phase. In uniaxial deformation mode totally 78% of the retained austenite is transformed and finally 29% of the retained austenite is transformed into the martensite for the shear type deformation mode.

In addition to results at the final stage of the deformations, the transformation is also investigated for the different prescribed displacements to evaluate the tendency of the retained austenite phases to transform into the martensite. This evaluation is only carried out for the tensile type deformation. In this part of the study, the grain sizes and shape helped us to comprehend the geometric effects on the martensitic transformations. In Fig. 9 the martensitic transformation is depicted for different displacement levels (Since all cases of the martensitic transformation cannot be depicted in Fig. 8, a video is also loaded to the system). As can be seen from the figure the first martensitic transformation initiate on the small and spherical type retained austenite. It's means that the stability of the retained austenite also depends on the shape and size of the retained austenite.

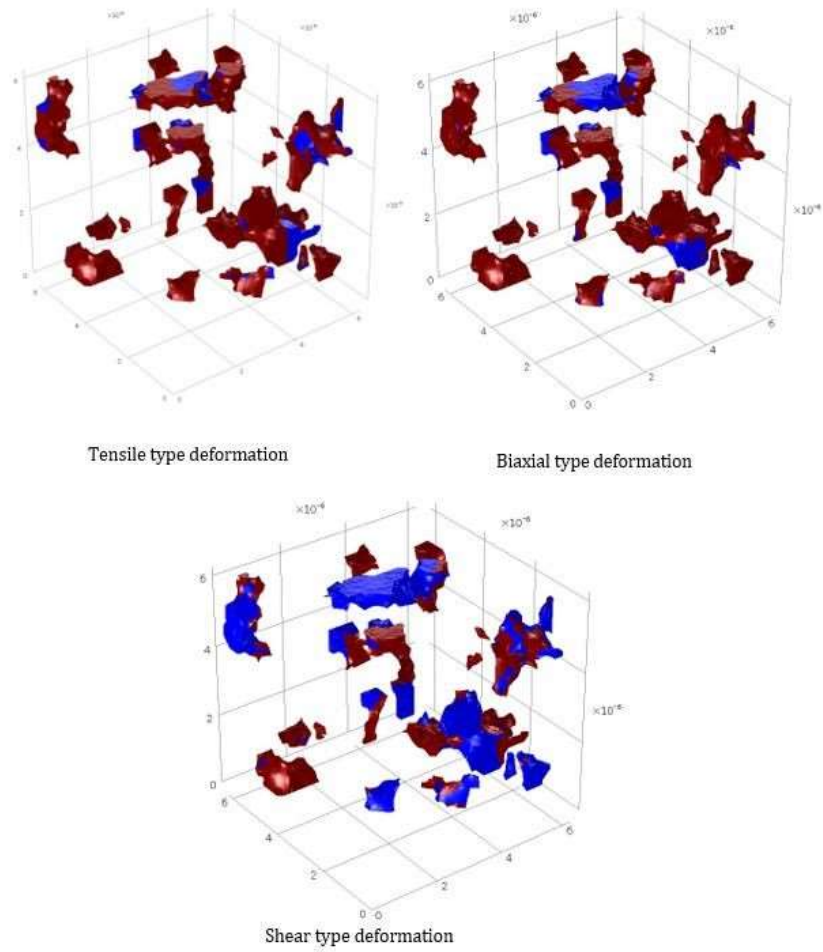


Fig. 8. Martensitic transformation under different loading conditions at $0.3 \mu\text{m}/\mu\text{m}$

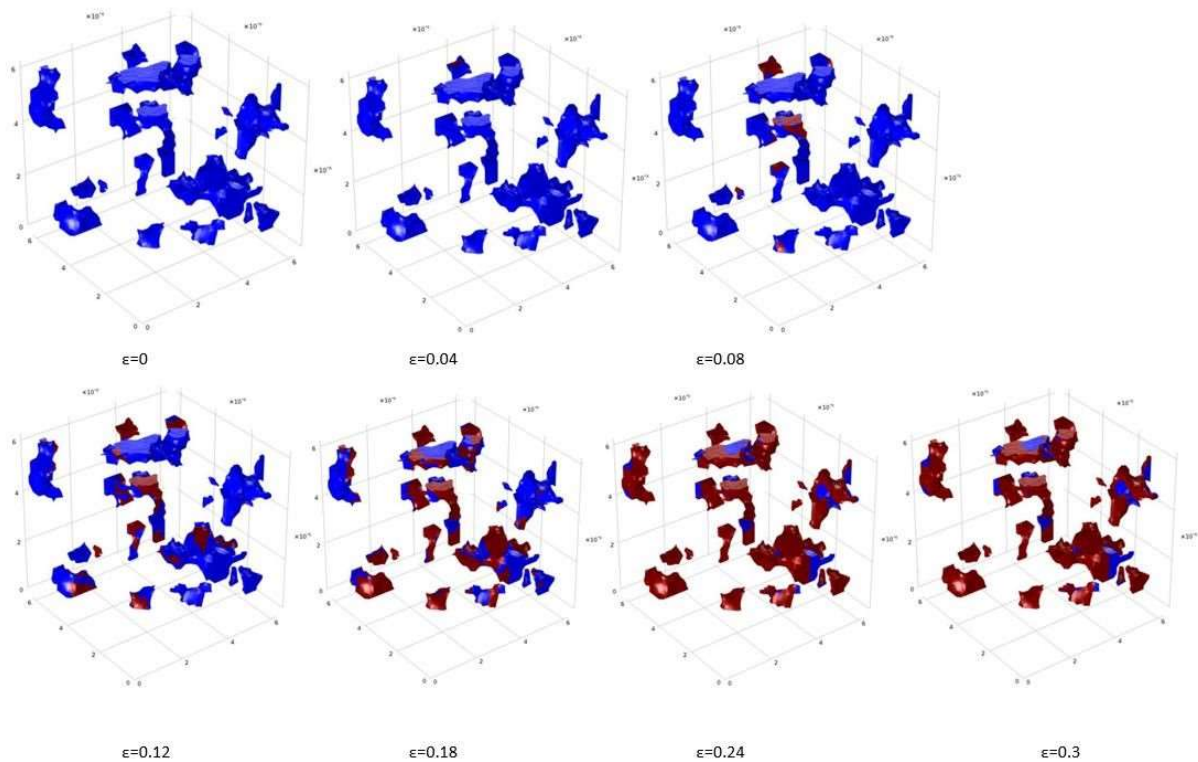


Fig. 9. Martensitic transformation for tensile type deformation modes at different strain levels ($0-0.3 \mu\text{m}/\mu\text{m}$)

5. CONCLUSIONS

The martensitic transformation of the advanced high strength TRIP800 (Transformation Induced Plasticity) steel is investigated in the microstructural level. A series of microstructural finite element simulations were carried out for tensile, biaxial and shear type deformation modes to determine the tendency of the retained austenite phases' transformation into the martensite. As a result, the synthetically generated microstructure which consist of 55% Ferrite, 35% Bainite and 10% Retained austenite show more tendency to transform into the martensite under biaxial loading conditions and approximately 86% of retained austenite transform into the martensite phase. Additionally the analyses depicts that the granular shape retained austenite phases are more eager to transform into the martensite.

References

- (Digital representation environment for analyzing microstructure in 3D. 8 ed. 2013. <http://dream3dbluequartznet>).
- Alveen, P., D. McNamara, D. Carolan, N. Murphy, A. Ivanković (2013). Micromechanical modelling of advanced ceramics, 13th International Conference on Fracture. China.
- Choi, K. S., A. Soulami, W. N. Liu, X. Sun and M. A. Khaleel (2010). Influence of various material design parameters on deformation behaviors of TRIP steels, *Computational Materials Science* 50(2): 720-730.
- Dan, W. J., W. G. Zhang, S. H. Li and Z. Q. Lin (2007). A model for strain-induced martensitic transformation of TRIP steel with strain rate, *Computational Materials Science* 40(1): 101-107.
- Davut, K. and S. Zaefferer (2012). The Effect of Size and Shape of Austenite Grains on the Mechanical Properties of a Low-Alloyed TRIP Steel, *Steel Research International* 83(6): 584- 589.
- Fischer, F. D., E. R. Oberaigner, K. Tanaka and F. Nishimura (1998). Transformation induced plasticity revised an updated formulation, *International Journal of Solids and Structures* 35(18): 2209-2227.
- Fischer, F. D., G. Reisner, E. Werner, K. Tanaka, G. Cailletaud and T. Antretter (2000). A new view on transformation induced plasticity (TRIP), *International Journal of Plasticity* 16(7-8): 723-748.
- Fu, Y. T., J. Liu, J. Shi, W. Q. Cao and H. Dong (2013). Effects of Cold Rolling Reduction on Retained Austenite Fraction and Mechanical Properties of High-Si TRIP Steel, *Journal of Iron and Steel Research International* 20(5): 50-56.
- Groeber, M., S. Ghosh, M. D. Uchic and D. M. Dimiduk (2008a). A framework for automated analysis and simulation of 3D polycrystalline micro structures. Part 1: Statistical characterization, *Acta Materialia* 56(6): 1257-1273.
- Groeber, M., S. Ghosh, M. D. Uchic and D. M. Dimiduk (2008b). A framework for automated analysis and simulation of 3D polycrystalline micro structures. Part 2: Synthetic structure generation, *Acta Materialia* 56(6): 1274-1287.
- He, Z. P., Y. L. He, Y. T. Ling, Q. H. Wu, Y. Gao and L. Li (2012). Effect of strain rate on deformation behavior of TRIP steels, *Journal of Materials Processing Technology* 212(10): 2141-2147.
- Jacques, P. J., E. Girault, A. Mertens, B. Verlinden, J. van Humbeeck and F. Delannay (2001). The developments of cold-rolled TRIP-assisted multiphase steels. Al-alloyed TRIP- assisted multiphase steels, *Isij International* 41(9): 1068-1074.
- Kubler, R. F., M. Berveiller and P. Buessler (2011). Semi phenomenological modelling of the behavior of TRIP steels, *International Journal of Plasticity* 27(3): 299-327.

Kubler, R., M. Berveiller, P. Buessler and X. Lemoine (2010). Semi Phenomenological Modelling of the Behaviour of Trip Steels-Application to Sheet Metal Forming, *International Journal of Material Forming* 3: 69-72.

Olson, G. B. and M. Cohen (1975). Kinetics of strain-induced martensitic transformation, *Metallurgical Transactions A* 6A: 791-795.

Sierra, R. and J. A. Nemes (2008). Investigation of the mechanical behaviour of multi-phase TRIP steels using finite element methods, *International Journal of Mechanical Sciences* 50(4): 649-665.

Stringfellow, R. G., D. M. Parks and G. B. Olson (1992). A Constitutive Model for Transformation Plasticity Accompanying Strain-Induced Martensitic Transformations in Metastable Austenitic Steels, *Acta Metallurgica Et Materialia* 40(7): 1703-1716.

Tjahjanto, D. D., A. S. J. Suiker, S. Turteltaub, P. E. J. R. D. del Castillo and S. van der Zwaag (2007). Micromechanical predictions of TRIP steel behavior as a function of microstructural parameters, *Computational Materials Science* 41(1): 107-116.

Tomita, Y. and T. Iwamoto (2001). Computational prediction of deformation behavior of TRIP steels under cyclic loading, *International Journal of Mechanical Sciences* 43(9): 2017- 2034.

Uthaisangsuk, V., U. Prahll and W. Bleck (2009). Characterisation of formability behaviour of multiphase steels by micromechanical modelling, *International Journal of Fracture* 157(1-2): 55-69.

Uthaisangsuk, V., U. Prahll and W. Bleck (2011). Modelling of damage and failure in multiphase high strength DP and TRIP steels, *Engineering Fracture Mechanics* 78(3): 469- 486.

Yu, H. Y., S. H. Li and Y. K. Gao (2006). Deformation behavior of the constituent phases for cold-rolled TRIP-assisted steels during uniaxial tension, *Materials Characterization* 57(3): 160-165.

Zrník, J., O. Stejskal, Z. Nový and P. Hornak (2007b). Relationship of microstructure and mechanical properties of TRIP-aided steel processed by press forging, *Journal of Materials Processing Technology* 192: 367-372.

Zrník, J., O. Stejskal, Z. Nový, P. Hornak and M. Fujda (2007a). Structure dependence of the TRIP phenomenon in Si-Mn bulk steel, *Materials Science and Engineering: A* 462(1-2): 253- 258.